Scanning Microscopy

Volume 4 | Number 3 Article 11

8-10-1990

Incorporation and Degradation of Hydroxyapatite Implants of Different Surface Roughness and Surface Structure in Bone

C. M. Müller-Mai
Freie Universität Berlin

C. Voigt
Freie Universität Berlin

U. Gross
Freie Universität Berlin

Scanning Microscopy, Vol. 4, No. 3, 1990 (Pages 613-624)
Scanning Microscopy International, Chicago (AMF O'Hare), IL 60666 USA

0891-7035/90$3.00+.00

Incorporation and Degradation of Hydroxyapatite Implants of Different Surface Roughness and Surface Structure in Bone

C.M. Müller-Mai*, C. Voigt+, U. Gross

Institute of Pathology and +Department of Traumatology and Reconstructive Surgery, Klinikum Steglitz, Freie Universität Berlin, Hindenburgdamm 30, D 1000 Berlin 45, FRG.

(Received for publication January 25, 1990, and in revised form August 10, 1990)

ABSTRACT

The interface of dense hydroxyapatite (HA) implants with different surface roughnesses was investigated after implantation into the spongy bone of the distal femur of rabbits by scanning electron microscopy (SEM) and transmission electron microscopy (TEM) following transverse fractures in the interface. Each implant displayed considerable changes in surface morphology caused by leaching (increasing pore diameter), corrosion (particulate disintegration), and active resorption by osteoclasts. Macrophages were involved in "cleaning" the surface via phagocytosis of loose implant particles. Newly formed surface elevations provided adhesion points for fibers and fibrils. Subsequent mineralization of these areas stabilized the interdigitation of surface elevations and extracellular matrix with adhering fibers and contributed to the tensile strength in the interface. This investigation provides further knowledge about HA implants, which seem to be partially resorbed by osteoclast-like cells.

Key words: Bone, Implant, Hydroxyapatite, Surface roughness, Resorption, Corrosion, Leaching, Degradation.

*Address for correspondence:
Christian M. Müller-Mai, Institute of Pathology, Klinikum Steglitz, Freie Universität Berlin, Hindenburgdamm 30, D 1000 Berlin 45, FRG. Phone: 030-798 2296.

INTRODUCTION

Bone-bonding to a variety of surface-reactive materials, such as glasses, glass-ceramics, and calcium-phosphate ceramics of different compositions is a well-known phenomenon (Gross and Strunz, 1985; Hench et al., 1971; Jarcho, 1981). The aim to achieve bone-bonding seems to depend - among other parameters - on the solubility of the material. If the solubility is too low, the material becomes covered with osteoid, chondroid, and soft tissue (Gross and Strunz, 1980). If the solubility is too high, implants will be degraded due to various processes (Gross et al., 1981; Hench and Ethridge, 1982). Resorbable materials, e.g. tricalcium phosphate and others, might enhance further biodegradation. This may occur by modification of the pH or by increased leaching and corrosion rates due to inhibited bone-bonding, as well as by active resorption through cells which are attracted by the implant. Calcium phosphate ceramics with a Ca/P-ratio below 1.2 produce a pH in an aqueous solution below the physiological pH of about 7.4. An acidic environment increases the solubility of Ca and might enhance further dissolution of Ca-containing implants (Bauer et al., 1989). Additionally, implant shape and surface roughness are extremely important. It has been shown that rough surfaces increased the inflammatory reaction at the implant surface (Salthouse, 1984). Other studies proved that osteoclasts, macrophages, and other cells, e.g. osteoblasts, are able to phagocytose and to solubilize intracellular implant particles in vitro (Kwong et al., 1989). To avoid serious inflammatory reactions, hydroxyapatites of different densities and porosities with a Ca/P ratio of 1.67 have been used, which is similar to that of human bone hydroxyapatite. Several studies proved that the stability of HA in a physiological environment is, among other parameters, dependent on the implant microporosity (de Groot, 1980; Klein et al., 1985). Concerning the degradation of HA implants, the current literature gives contradicting information. Some authors could not observe that dense HA is degraded (Denissen et al., 1980; Hoogendoorn et al., 1984), while others proved that there is some degradation

with a macrophage layer at the interface (Winter et al., 1981).

To get further information about the interaction of HA implants and a bony implantation bed, dense and highly pure HA implants produced by hot isostatic pressing (HIP) of different surface roughness and surface structure and a flame sprayed HA-coating on titanium cylinders with a certain porosity were examined with the scanning electron microscope (SEM) and transmission electron microscope (TEM), using a standardized animal model (Müller-Mai et al., 1989). The interface was examined after performing transverse fractures to achieve ultrastructural information about bone-bonding mechanisms, the changes in implant surface morphology, and processes of implant degradation due to leaching, corrosion, and resorption. The term bone-bonding which is used in this study, refers to intimate bone-implant contact which was demonstrated morphologically and which was documented in performing tensile strength tests (Müller-Mai et al., 1989).

MATERIALS AND METHODS

Cylinders of pure hydroxyapatite (6 mm long, 4 mm in diameter) with different surface roughnesses and metal rods coated with different hydroxyapatites were implanted into the trabecular bone of the distal femur epiphysis of female Chinchilla rabbits (average weight 3500g). The implants had been sterilized by gamma-irradiation and were inserted in a sagittal direction with their longitudinal axis perpendicular to the long axis of the femur. The trabecular bone behind the patellar sliding plane was reamed to 3.95 mm with a diamond-coated hollow cylinder drill at low speed under a constant flow of physiological NaCl-solution for cooling through the hollow cylinder drill by a pump. The animals were given 20 mg gentamycin and 0.5 ml Bela-Parm Antiphlogisticum 30% (Bela Pharm KG, Vechta, FRG) before operation. A ketaminhydrochloride/ Rompun^{R} (Bayer, Leverkusen, FRG) mixture (25 mg and 5 mg per kg body weight) was used for anaesthesia. All of the implants were incorporated without disturbance of the healing sequence. No implant was lost, e.g. due to infection. The rabbits were fed with Altromin^{R} standard diet hard pellets (Altromin, 4937 Lage-Lippe, FRG) and water ad libitum. They were sacrificed 84 and 168 days after implantation in anaesthesia by perfusion via the abdominal aorta with 80 ml glutaraldehyde 4% in 0.1 M cacodylate buffer pH 7.2 at 4°C for 5-10 minutes after a single dose of 10 mg Regitin^{R} for 30 seconds (Ciba, Wehr, FRG). Regitin^{R} is a smooth muscle relaxant and was used to enhance fixation efficacy. Both of the solutions mentioned above were applied using a syringe under manual pressure via a Butterfly^{R}-21 (Venisystems^{TM}, no. 4432, Abbott Ireland LTD., Ireland).

The following HA implants and coatings, respectively, were introduced into this investigation:

Cylinders of dense HA were produced by hot isostatic pressing (HIP, by Battelle-Institute, Frankfurt, FRG). This manufacturing process provided a density of almost 100% (d = 2.97 to 3.03 g/cm^3). By grinding and polishing the implant surface with diamond HA HIP RZ 0.5 μm (n = 32) was produced (DIN 4768). Surface roughnesses of RZ 20 μm (n = 32) and RZ 50 μm (n = 34) were produced by corundum particle blasting of different size after grinding.

Titanium cylinders with HA RT 50 μm coating (DIN 4762/1E) were produced by the plasma spraying technique (by Aesculap AG, Tuttlingen, FRG; n = 32). Due to the relatively high residual porosity and the poor mechanical strength of this coating it is not possible to produce defined and graduated surface roughnesses by means of mechanical treatment. So the "as-plasma-sprayed-surface" had to be used. It can be varied only within narrow limitations by variation of the plasma spraying parameters.

CoCrMo-cylinders (ISO 583/IV) were coated with HA HIP RZ 0.5 μm (n = 24) by means of the above mentioned HIP-technique and polishing (Battelle-Institute, Frankfurt, FRG). The coatings were 100% dense and had a thickness of about 200 μm.

It must be pointed out, that the physico-chemical and the biological properties of HA implants depend on the manufacturing technique and surface treatment of the materials. The HA produced by HIP has a significant high density and uniform phase composition by X-ray diffraction analysis. Foreign phases such as tricalciumphosphate and tetracalciumphosphate could not be detected. The HA flame sprayed coatings had a certain amount of tricalciumphosphate and tetracalciumphosphate which could be detected by X-ray diffraction analysis. The exact evaluation of phase compositions of such HA-materials is an, as yet, unsolved problem. It is nearly impossible to detect cryptocrystalline and amorphous phases such as glasses and intergranular secondary phases which can obviously influence the materials behaviour in a bony implantation bed. Contradictary biological findings in the literature may result from this.

All implant types were subjected to light microscopy, histomorphometry, and tensile testing after explantation, the results of which will be shown in another report. One implant of each type was explanted after 84 and 168 days, fractured at the tissue/implant interface (see below). One part of the distal interface - tissue and the remaining implant cylinder were examined by SEM and the other part of the distal interface - tissue with adherent HA-material by TEM. The mean pore and HA-grain diameters were measured in the interface using the SEM specimens. For comparison, diameters of pores and grains were measured on fracture planes in the HA-material which were produced by transverse fractures and which were not directly exposed to the tissues (Fig.1). It must be emphasized that due to the preparation process, evidence cannot be given here for the distance between fracture plane and interface.

After opening of the knee-joint of the perfused animals the implants were exposed on

the ventral side using a diamond-coated saw disk. Five cuts were necessary before the tissue, which was tightly adhering to the implant surface, could be removed by performing transverse fractures in the distal interfaces. The distal interface was chosen for preparatory reasons and because of the load transmitted here. The cuts were executed parallel to the longitudinal axis of the implant from medial, lateral, and caudal. The caudal-lateral and the caudal-medial pieces were cut again in the middle. By breaking off the two distal pieces of the four-eighths of the tissue, which were produced by the five cuts, it was possible to lay open the distal interface. Then the collected specimens of implant (Fig.2) and tissue (Fig.3) were immediately rinsed in physiological saline solution and fixed in glutaraldehyde 4% in 0.1 M cacodylate buffer, pH 7.2 at 4° C. Afterwards, they were rinsed in cacodylate buffer (see above) for 3 x 5 minutes and dehydrated in graded ethanols (30%, 50%, 70%, 80%, 90%, 96%, 3 x absolute ethanol) for 30 minutes each. The specimens were dried using the critical point method, glued on aluminium stubs, sputtered with gold-palladium and analysed with a Philips SEM 505 scanning electron microscope.

The TEM specimens were fixed with glutaraldehyde 4% in 0.1 M cacodylate buffer pH 7.2 at 4°C for 2 hours. This was followed by rinsing with cacodylate buffer (see above) for 3 x 15 minutes and postfixation with OsO_4 1% in cacodylate buffer at 4°C overnight. Then the specimens were rinsed with veronal buffer pH 6.0 for 3 x 5 minutes and stained with 0.5% uranylacetate in veronal buffer for 1 hour at 4°C. This was followed by dehydration in graded ethanols (70%, 80%, 90%, 96%, 3 x absolute ethanol, 15 minutes each), soaking with 1.2 propylene oxide (3 x 5 minutes), embedding with propylene oxide Spurr's low-viscosity resin mixture 1:1 overnight, Spurr's resin concentrated for 2 hours. After changing Spurr's resin, the polymerization of the specimen/Spurr mixture in gelatine capsules in a vacuum at 70°C followed. The hardened specimens containing material were glued to metal stubs and sawed with a sawing microtome (Leitz 1600, Leitz-Wetzlar, Wetzlar, FRG) perpendicular to the longitudinal axis of the implants. The slices were approximately 500 μm thick. The specimens were examined under a light microscope after using the Richardson technique which produces strong staining of glutaraldehyde and OsO_4 fixed tissues to detect interface structures of interest and then embedded in Spurr's resin. Interesting sides were freed from resin and HA-material, first by using a sawing microtome, and then by filing until just a thin layer of the implant was left. Ultrathin sections were cut with an Ultracut E Microtom (Reichert-Jung) perpendicular to the interface. Poststaining was carried out with 4% uranyl-acetate for 10 minutes at 60°C. The specimens were rinsed and dried, stained with lead citrate (5%) and washed again. The examinations were performed with a Philips EM 410 TEM.

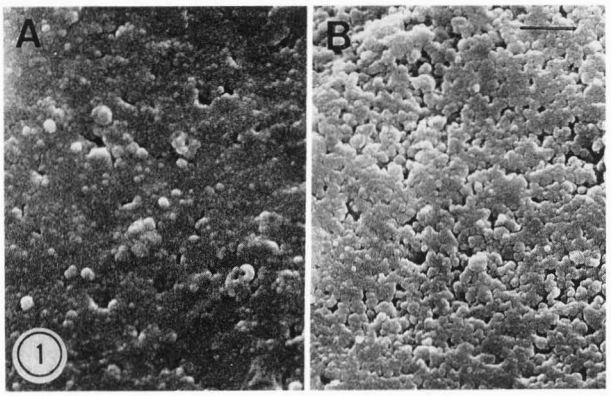

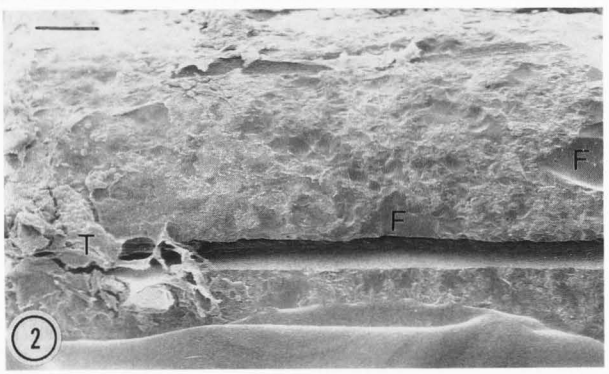

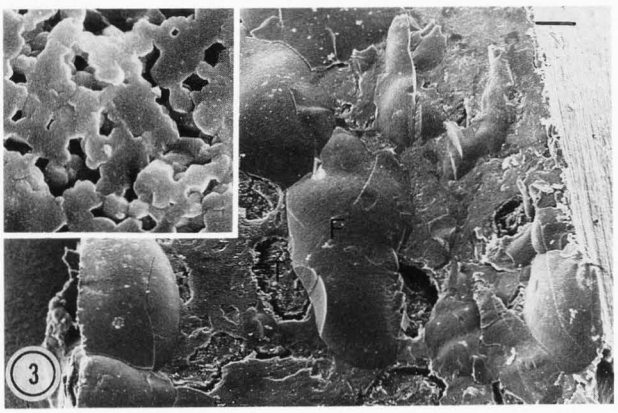

Fig. 1: Microstructure with pores and grains of a HA HIP RZ 50 μm implant 84 days after implantation, A Fracture plane, B interface. SEM, bar 0.4 μm.

Fig. 2: Fracture in the distal interface of a HA HIP RZ 50 μm implant 168 days after implantation. Adhering tissue (T), fracture planes (F) and grooves due to preparation. SEM, bar 300 μm.

Fig. 3: Tissue side of a HA HIP RZ 0.5 μm implant 168 days after implantation with adhering implant material showing fracture planes (F). Soft tissue and bone marrow (T) free of HA. Inset with microstructure of HA fracture plane. SEM, bar 100 μm, inset 0.5 μm.

RESULTS

Hydroxyapatite HIP RZ 0.5 μm

Eighty-four days after implantation, there were areas in which HA particles adhered to the tissue after transverse fracturing. TEM revealed bone-bonding areas with dense bundles of mineralized collagen fibers, whose longitudinal axes ran mostly parallel to the interface. In non-bonding areas, there were fibroblasts and occasionally a few macrophages at the interface. This cellular layer was followed by collagen-rich extracellular matrix with some capillaries and macrophages. Some of these macrophages contained phagocytosed implant material (Fig.4). The average pore diameter of the material was between 0.06 μm (fracture plane) and 0.22 μm (interface) (Table 1). Single HA grains could be discriminated and had an average diameter of 0.29 μm in the interface and 0.31 μm in fracture planes (Table 2). At higher magnifications, TEM revealed some HA-grains of non-bonding surface areas which were covered with a microscopic layer of needle-like crystals. This layer had a width of approximately 60 nm.

After 168 days of implantation, the interface could hardly be exposed by fracture. Large particles of hydroxyapatite adhered to the tissue. They had been broken off, producing areas of so-called shell-fractures (Fig.3). In the fracture plane, these particles displayed single pores with an average diameter of 0.19 μm (Table 1). The single grains of the hydroxyapatite were also visible and had an average diameter of approximately 0.34 μm (Table 2). Only a few areas of the tissue side of the interface were free from hydroxyapatite particles. These areas consisted exclusively of tissue which was rich in bone marrow and fibers, with some round cells. In TEM, all ultrathin sections showed mineralized bone in the interface, which had been growing in the micropores between the grains (Fig.5). From these findings, a bone-implant-bonding can be deduced which shows a higher stability of the interface than of the implant material or surrounding tissue.

Hydroxyapatite HIP RZ 20 μm

The implants that had been explanted after 84 days showed extensive particles which were broken off the implant in the shape of shell-fractures and adhered to the tissue side. On the fracture planes of the broken-off hydroxyapatite, the typical pores could be observed. In the interface, pores had a diameter

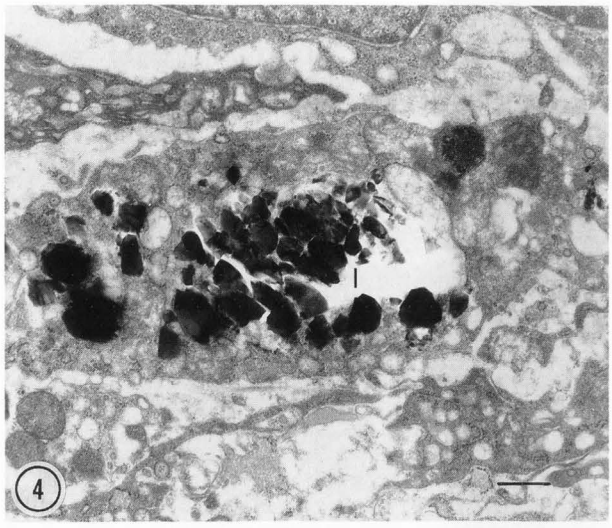

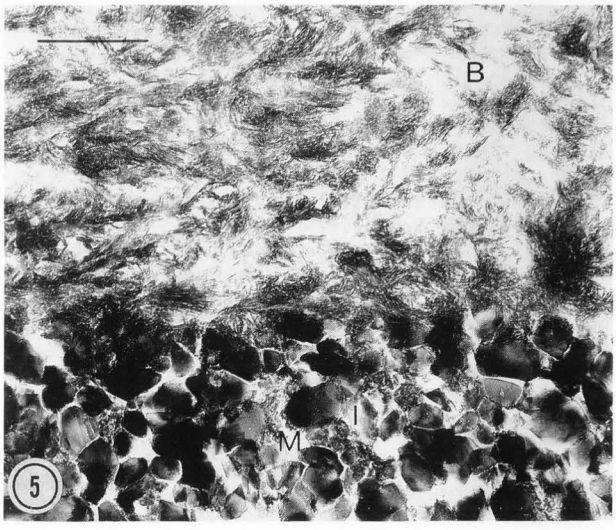

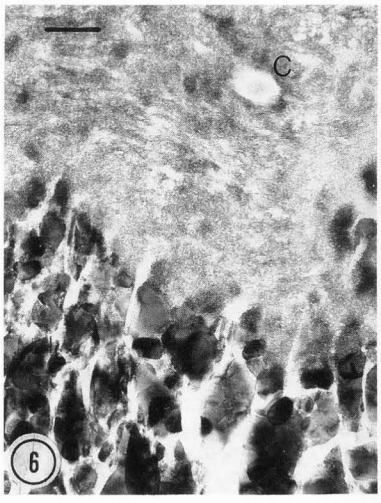

Fig. 4: Cell with phagocytosed implant material (I) in the vicinity of HA HIP 0.5 84 days after implantation. TEM, bar 0.5 μm.

Fig. 5: Bone-bonding area of HA HIP 0.5 μm implant 168 days after implantation. Mineralization (M) proceeds into the pores. Bone (B), implant (I), TEM, bar 0.5 μm.

Fig. 6: Bone-bonding area of a HA HIP RZ 20 μm implant 84 days after implantation. Mineralization between superficial HA grains. Canaliculus (C). TEM, bar 0.4 μm.

Table 1: Average size of the micropores (μm + standard deviation) of hydroxyapatite (HA) implants with different surface roughness at interface regions and on fracture planes after implantation into the trabecular bone of the distal femur epiphysis of rabbits. M = material, FP = fracture plane, HIP = hot isostatic pressing, RZ = surface roughness (μm), n = number of measured pores.

		pore size (μm)			
M (RZ)	days	n	interface	n	FP
HA HIP	84	25	0.220 ± 0.10	15	0.055 ± 0.02
(0.5)	168	11	0.197 ± 0.08	40	0.189 ± 0.09
HA HIP	84	15	0.115 ± 0.02	15	0.112 ± 0.06
(20)	168	25	0.168 ± 0.05	20	0.133 ± 0.04
HA HIP	84	20	0.093 ± 0.03	20	0.051 ± 0.02
(50)	168	25	0.131 ± 0.04	15	0.081 ± 0.03
HA HIP on CoCrMo (0.5)					
	84	20	0.124 ± 0.05	no pores visible	
	168	25	0.099 ± 0.04	25	0.062 ± 0.03

Table 2: Average size of HA-grains (μm ± standard deviation) of hydroxyapatite (HA) implants with different surface roughness at interface regions and on fracture planes after implantation into the trabecular bone of the distal femur epiphysis of rabbits. M = material, FP = fracture plane, HIP = hot isostatic pressing, RZ = surface roughness (μm), n = number of measured grains.

		grain size (μm)			
M (RZ)	days	n	interface	n	FP
HA HIP	84	20	0.294 ± 0.09	20	0.309 ± 0.12
(0.5)	168	6	0.264 ± 0.05	30	0.342 ± 0.11
HA HIP	84	30	0.197 ± 0.07	10	0.301 ± 0.03
(20)	168	25	0.329 ± 0.09	35	0.409 ± 0.15
HA HIP	84	30	0.123 ± 0.04	10	0.175 ± 0.04
(50)	168	25	0.115 ± 0.03	10	0.152 ± 0.02
HA HIP on CoCrMo (0.5)					
	84	20	0.151 ± 0.03	not detectable	
	168	25	0.125 ± 0.05	15	0.287 ± 0.03

of 0.12 μm (Table 1) and the grains 0.2 μm (Table 2). TEM revealed large areas of the implant surface which were covered mainly with mineralized collagen fibers aligned parallel to the interface (Fig.6). These fibers formed a thin mineralized layer on the material surface. This layer was covered with osteoblasts or collagen-rich soft tissue with capillaries and a few macrophages. Some macrophages contained phagocytosed implant particles. In a few areas the soft tissue containing macrophages reached the implant surface.

After 168 days of implantation, most of the ultrathin sections showed mineralized collagen fibers in parallel covering the HA-surface. Only a few areas showed fibrocytes in the interface, some of which touched the HA-surface with their cellular membrane, and some of which were seperated by an amorphous extracellular matrix with only a few fibers (Fig.7). In interface areas, the mean pore diameter was larger and the grain diameter was smaller than on fracture planes (Tables 1, 2).

Hydroxyapatite RZ 50 m

After performing a transverse fracture in the interface, the general overview of the implant showed a relatively smooth surface with impressions and elevations and without sharp edges 84 days after implantation. In higher magnifications a microporosity of the implant was just visible (diameter of interface pores 0.09 μm and of fracture plane pores 0.05 μm, Table 1). The surface showed an evenly spaced roughening which could have been created through leaching and corrosion. In such areas, the individual hydroxyapatite grains, some of which seemed to have been lost, were easy to distinguish (Fig.1 B). Many single HA-particles could be found loosely scattered in the extracellular matrix (ECM) in the TEM sections. Some particles had been phagocytosed by macrophages and occasionally by osteoblast-like cells (Fig.8). In one surface area, a multinucleated giant cell could be observed on the surface of the material (Figs.9,10). Between highly convoluted cellular membrane and bulk material some loose single implant grains could be found. In similarily modified areas, SEM revealed many thick nets of fibers which were anchored to the newly created rough surface by interdigitating with the HA grains. Some fibers displayed distensions in some sections, which could be an equivalent to a mineralization of collagen fibers. These nets of fibers covered large surface areas and partly created structures resembling trabeculae. In the TEM sections nearly the whole HA-surface was covered by mineralized tissue which either showed trabecular structures or formed just one layer of mineralized collagen fibers of less then 1 μm width. The tissue side was almost completely covered by adhering hydroxyapatite particles in areas of bone trabeculae. The HA-grains of these fracture planes had an average diameter of 0.18 μm (interface 0.12 μm, table 2). These adhering particles displayed surfaces which resembled shell-fractures. There were areas without implant material between the

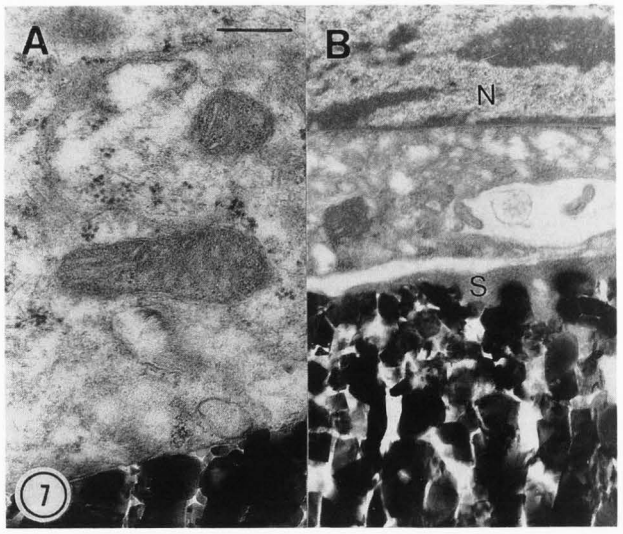

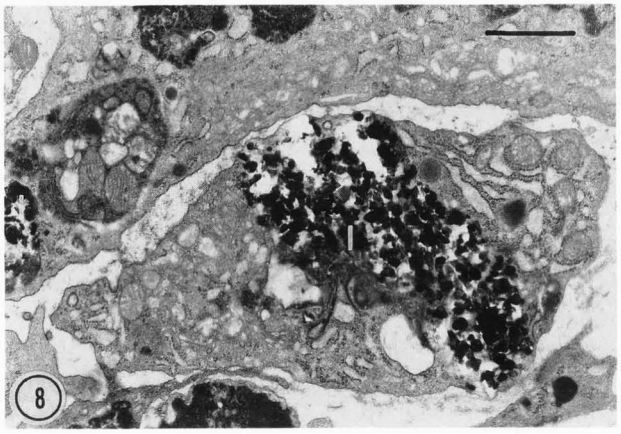

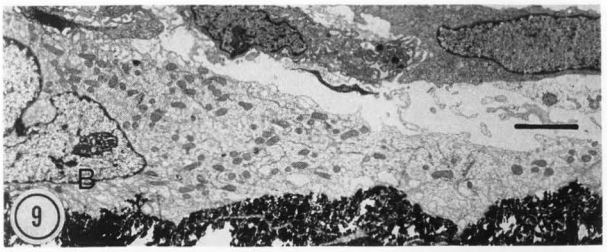

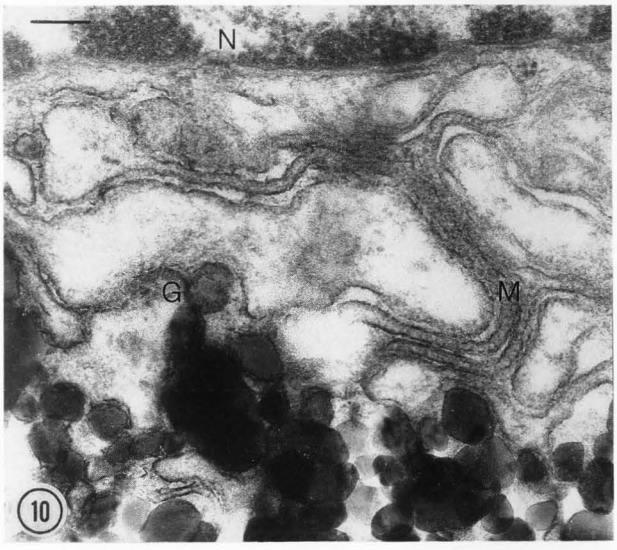

Fig. 7: Different aspects of non-bonding areas in the interface: A shows a cellular membrane in direct contact with the HA implant. In B the fibrocyte's membrane is separated from the implant by an amorphous seam (S), nucleus (N). TEM, bar 0.3 μm (A), 0.8 μm (B).

Fig. 8: Cells with phagocytosed implant material (I) in the vicinity of a HA HIP RZ 50 μm implant 84 days after implantation. TEM, bar 1 μm.

Fig. 9: Multinucleated giant cell with a folded cellular membrane (B) on the surface of a HA HIP RZ 50 μm implant 84 days after implantation. TEM, bar 2 μm.

Fig. 10: High magnification of Fig. 9. Note the highly folded cellular membrane (M) and grain of implant origin (G) which has lost contact to the bulk material, nucleus (N). TEM, bar 0.2 μm.

hydroxyapatite particles which remained on bone trabeculae, especially bone marrow and soft tissue. Because of the adhesion between implant and trabecule a bone-bonding effect can be assumed.

After 168 days of implantation, large shell-fracture-like, broken-off hydroxyapatite particles could be observed which adhered to the tissue side. The actual interface laid open only in a few places. Besides the characteristic impressions and elevations with the above-mentioned pores and grains (pore diameter in the interface 0.13 μm, grain diameter 0.12 μm) (Tables 1, 2), areas with roughened surface of up to 100 μm in diameter were visible. These areas formed new impressions of the surface. Often, nets of fibers were attaching and woven into these newly-formed micro-roughnesses. These roughnesses could only be found on interface areas which laid open. Therefore, they were probably induced by tissue reaction. Here, the individual hydroxyapatite grains were easy to distinguish, which was apparently due to a loss of particles which had been lying between them. This phenomenon points to a superficial release of particles (corrosion), i.e. a particulate disintegration. In these areas, the average pore diameter rose to about 0.2 μm while the average grain diameter sank to about 0.1 μm. Thus, three processes seemed to have had a synergistic effect leading to a modification of the implant surface structure:

- -leaching, as shown by an increasing pore diameter and a decreasing grain diameter;
- -particulate disintegration, i.e. the loss of hydroxyapatite grains;
- -resorptive phenomena, e.g. through macrophages or osteoclasts.

Hydroxyapatite flame spray RT 50 μm

After 84 days of implantation, several larger tissue components could be found on a

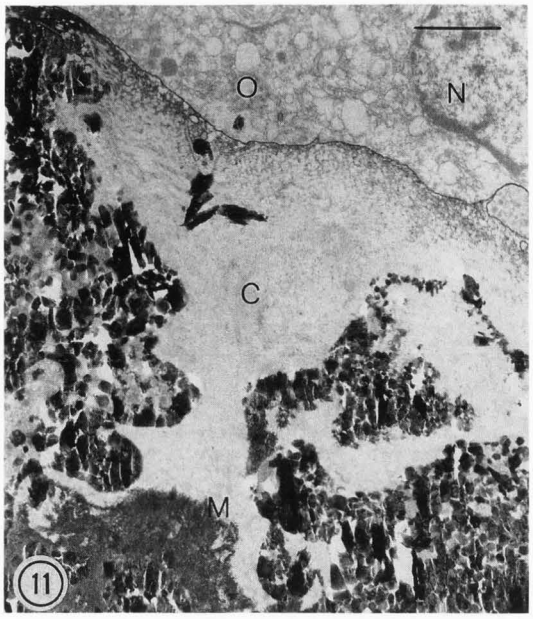

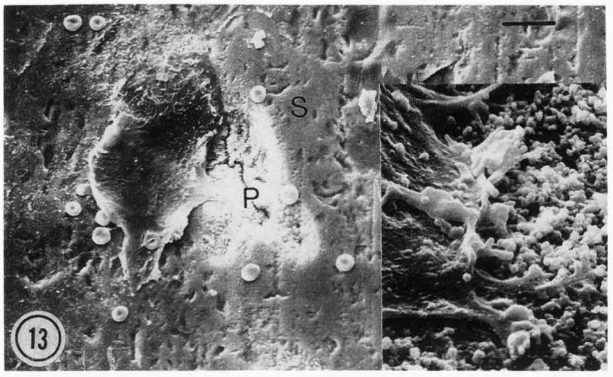

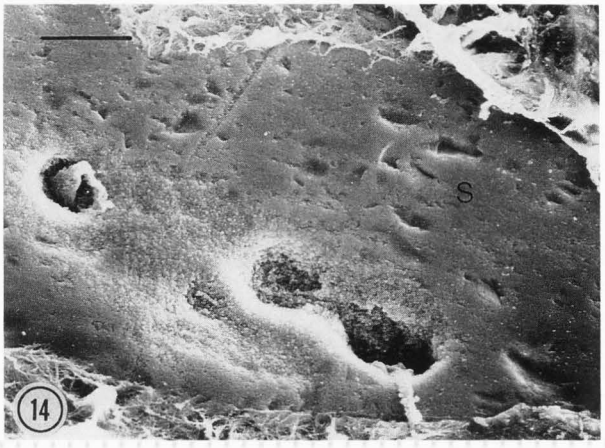

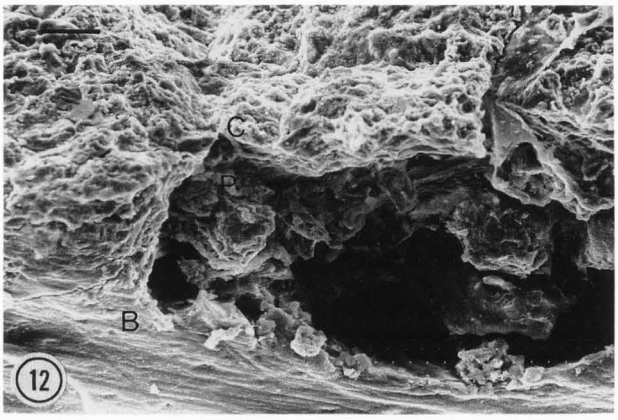

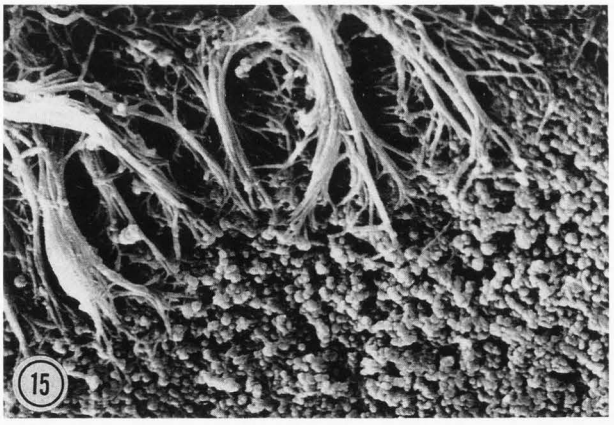

Fig. 11: Interface of a titanium cylinder flame sprayed with HA 50 μm 84 days after implantation. The surface roughness is bridged by a collagen-rich ECM (C) which is already partially mineralized (M). The tissue side of the ECM is relatively smooth and covered with osteoblasts (O), nucleus (N). TEM, bar 2 μm.

Fig 12: Tissue side of a titanium cylinder flame sprayed with HA RT 50 μm 168 days after implantation. Flame-spray coating (C) almost completely adhering to the bone (B). Pit (P) in the coating at soft tissue area at the transition from bone to the implant surface. SEM, bar 20 μm.

Fig. 13: Resorbing giant cell on the surface of a CoCrMo cylinder coated with HA HIP RZ 0.5 μm 84 days after implantation. Relatively unchanged surface (S) and newly created pit (P). Inset with process of the giant cell extending into the pit. Note the scalloped appearance of the lower left of the pit. SEM, bar 10 μm, inset 1 μm.

Fig. 14: Relatively unchanged surface (S) of a CoCrMo-cylinder coated with HA HIP RZ 0.5 μm 168 days after implantation with adhering tissue (top, bottom), and newly created pits, one containing remnant of a cellular process (left). SEM, bar 10 μm.

Fig. 15: Newly created surface roughness on the surface of a CoCrMo cylinder coated with HA HIP RZ 0.5 μm 168 days after implantation with interdigitation of fibers. SEM, bar 1 μm.

titanium cylinder with flame-sprayed hydroxyapatite coating. Therefore, the anchoring of these tissue components to the implant seemed to be stronger than the connection to the tissue. Some tissue areas displayed trabecule-like structures with lamellar layers of mineralized collagen fibers and interspersed osteocytes. In the TEM sections, the implant surface was mostly covered by parallel mineralized fibers bridging the surface roughness. The surface of this mineralized seam on the implant was smooth on its tissue side and covered by a thin layer of collagen-rich ECM, which contained a number of matrix vesicles and calcospheritic structures. The ECM-layer was covered with osteoblasts (Fig.11). Between the tissue components, there were jagged projections of the implant surface, which showed small needle-like and crystal-like structures of up to 0.5 μm length and about 0.1 μm width. In other places, there was typical bone marrow tissue composed of round cell-like elements in a network of fibers between the elevations of the implant. An extracellular matrix consisted mainly of fibrillar structures, which served as an anchoring of cells to the material surface, and of globular and crystalline structures. The implant surface was remarkably smooth in some areas without contact to trabecular tissue components. No needle-like or crystal-like structures were present in these areas. Such surfaces could have been created by leaching, e.g. contact with intercellular fluid or with soft tissue. Some single HA-particles could be found in the ECM of TEM sections, indicating release of particles (corrosion).

After 168 days of implantation, it was hardly possible to expose the interface by trying to break apart implant and tissue. The fractures always took place within the implant material or, occasionally, within the tissue. The hydroxyapatite coating almost completely adhered to the tissue (Fig.12). There were only rare exceptional cases in which bone marrow tissue was not totally covered by adhering HA. These results indicate a tight bone-bonding to the hydroxyapatite coating. Newly formed impressions of the HA-surface in areas of soft tissue contact could be observed in cross-sections of the tissue and the HA-coating. In the TEM sections, some macrophages contained phagocytosed implant material.

Hydroxyapatite HIP RZ 0.5 μm coating on CoCrMo

Eighty-four days after implantation, many well-preserved surface areas were observable in the interface after fracture. These interface areas showed evenly distributed roundish impressions, the surfaces of which seemed to be extremely rough compared to the surrounding hydroxyapatite. One of these impressions with a scalloped outline contained a process of a giant cell which was more than 50 μm wide and displayed a folded cellular membrane, thus being an osteoclast (Fig.13). There were areas with broken-off, shell-fractured hydroxyapatite particles between well-preserved interface areas and newly formed impressions with surface roughnesses, which seemed to have been created by leaching, release of particles (corrosion), and resorption. These particles were discernible on the corresponding tissue side. The above mentioned porosity of the implant material was not visible on these fracture planes, and thus the implant density was almost 100%. Pores with a diameter of 0.12 μm could be found in interface areas (Table 1), and single HA-grains could therefore be distinguished (diameter 0.15 μm) (Table 2). There were hardly any exposed bone trabeculae on the tissue side. They were mostly covered by a thin hydroxyapatite layer. Exposed tissue areas consisted mostly of bone marrow or soft tissue.

After 168 days of implantation, the implant cylinder was well-preserved despite fracturing in the interface. Therefore, the implant cylinder could be totally recovered, showing only some superficial shell-like fractures in the HA-coating. At the proximal pole of the implant material, there was an almost vertically inserting bone trabecule on the implant surface. At the transition between trabecule and implant surface, a resorbing giant cell was found which was identified as an osteoclast by its typical brush border. On the hydroxyapatite surface, evenly distributed roundish impressions had a diameter of about 10 μm (Fig.14). They could be observed especially in the proximal-dorsal part, while there were fewer in the proximal-ventral and in distal parts. Especially areas of the newly formed surface roughness showed dense nets of fibers joining the hydroxyapatite (Fig.15). There were areas of soft tissue with interspersed fat cells and bone marrow between the attaching bone trabeculae. Next to exposed interface areas, the above mentioned typically fractured areas of the implant material could be observed. Accordingly, thin hydroxyapatite particles were visible on the corresponding tissue side and were almost exclusively connected to bone trabeculae. Intermediate marrow gaps showed no remains of the implant material. The implant showed the typical grains and pores, with a mean pore diameter in the interface of 0.1 μm and a mean grain diameter of 0.13 μm (Tables 1, 2).

DISCUSSION

An ideal implant material should allow the development of normal host tissue in the interface, and the reaction to physical stimuli and the remodeling should be like that of the tissue it replaces (Hench and Ethridge, 1982). It could be shown in this study, that all of the HA implants used develop bone and bone marrow in the interface and are attacked at their interfaces due to various processes, i.e. leaching, release of particles (corrosion), and resorption. There have been some contradicting studies stating that sintered HA displayed no resorption (Denissen et al., 1980; Hoogendoorn et al., 1984; Klein et al., 1983). In the first study (Denissen et al., 1980), this might be related to the implantation model (cortical bone). Since the latter two studies (Hoogendoorn et al., 1984; Klein et al., 1983) were performed using light microscopy, it is assumed that the resolution was not high enough to detect changes of surface morphology. It was shown in the present study, however, that in most of the

implants the pore diameter increases and the grain diameter decreases with time. Additionally, the pore diameter was larger in interface areas of all of the investigated implants than in fracture planes and the grain diameter was larger in fracture planes which were not directly exposed to the tissues. It must be emphasized that these data represent a trend only. Because of the small number of implants it was not possible to measure pore and grain diameters before implantation. However, these data are well in accordance with another study using different biphasic calcium phosphates as periodontal implants (Daculsi et al., 1989). Leached implant ions might participate in the crystallization process which takes place solely on the HA surface, and which leads to a coating of the implant with a microscopic layer of apatite (Jarcho, 1981). A similar microscopic layer could be observed in this study. Independent of the surface roughness, small particles of implant origin could be found scattered in the ECM or phagocytosed by macrophages. This was also described by other investigators using different implant models (Becker et al., 1987; van Blitterswijk et al., 1986; Klein et al., 1985; Winter et al., 1981). It was shown in an in vitro model that macrophages, osteoclasts, and to some extent osteoblasts were able to solubilize intracellular HA particles. When particles had a diameter of more than 50 μm, internalization and dissolution did not occur (Kwong et al., 1989). This fact points to the importance of leaching and release of implant particles (corrosion), that can be phagocytosed and dissolved. Therefore, it seems likely that especially macrophages which are loosely scattered in the collagen-rich ECM play a central role in "cleaning" the implant surface. Additionally, giant cells of about 50 μm in length could be detected in this study which had processes with a brush border extending into newly formed pits of the implant surface. This indicates active resorption of HA implant material by osteoclasts. A similar tissue reaction was described using tricalcium phosphate plates in the hypotympanon (Büsing et al., 1987). The newly created pits on the HA surface showed obvious micro-roughnesses which were typical for these surfaces. The diameter of the grains forming the micro-roughness corresponded with the diameter of single implant HA grains. In another light microscopic study using titanium rods flame-sprayed with HA, the coating showed newly formed depressions typically formed at the transition from trabeculae to the implant surface. It was speculated in this previous study that the active production of these pits by osteoclasts might produce a homogeneous surface stress state at the bone-implant transition by this surface profile to prevent localized stress peaks (Gross et al., 1989). A similar situation could be demonstrated in the present study, especially at the proximal-dorsal pole of a CoCrMo-cylinder coated with HA HIP RZ 0.5 μm. In the normal rabbit femur without implant, this is an area of bone marrow which might be the source of increased resorption. These results demonstrate that HA implants show a time-dependent change in surface morphology. This behavior has been observed for other surface-reactive materials, e.g. KG Cera glass-ceramic. It was shown that this material develops a surface roughness which enables cells and fibers to adhere and is partially remodeled like bone (Gross et al., 1988a and 1988b). When a roughened area becomes mineralized, the interdigitation of fibers and implant surface roughness contributes to the tensile strength in the interface which was measured in other studies (Müller-Mai et al., 1989). A similar situation has been observed in studies using active bioglasses in which collagen fibers became incorporated in the newly formed Si-Ca/P-film on the implant surface (Davies and Matsuda, 1988; Matsuda and Davies, 1987).

In systematic studies using implants of different microporosity and macroporosity, as well as different crystallographic structure, it was concluded that the rate of degradation of calcium phosphate implants is related to the content of pores, the total density, the crystallographic structure of the implant material, and the Ca/P-ratio (de Groot, 1980; Klein et al., 1983, 1985, 1986; Köster et al., 1976). Pores seem to be important for the degradation rate especially in non-bonding areas. If there is bone-bonding, macropores and micropores seem to contribute to implant fixation due to bone-ingrowth, which was demonstrated here and in a former study (Kato et al., 1979).

In conclusion, three synergistic effects seem to contribute to the degradation of HA bone-implants. Starting with the insertion, the implant is attacked by leaching processes related to the tissue which is in contact to the implant surface. Macropores and micropores determine the number of grain boundaries in the implant. Leaching causes loss of HA grains, leads to release of particles (corrosion), and induces phagocytosis and intracellular solubilization of implant particles. Osteoclasts are able to modify the HA implant surface by active resorption.

Acknowledgements

This study was supported by the Ministry for Research and Technology, Bonn, FRG, grant 01 VG 8603. For advice we are grateful to H. Heide, Battelle-Institute, Frankfurt, FRG. The material was provided by Battelle-Institute, Frankfurt, FRG and Aesculap, Tuttlingen, FRG.

REFERENCES

Bauer G, Donath K, Dumbach J, Kroha E, Sitzmann F, Spitzer WJ, Stiegelschmitt A (1989) Reaktion des Knochens auf Kalziumphosphatkeramiken unterschiedlicher Zusammensetzungen. Z. Zahnärztl. Implantol. 5 263-266.

Becker J, Kuntz A, Gross U, Fensch FE, Küpper W, Reichart P (1987) Tierexperimentelle Untersuchungen zur Einheilung von Zahnwurzelimplantaten aus Hydroxylapatit. Z. Zahnärztl. Implantol. 3 200-205.

van Blitterswijk CA, Kuijpers W, Daems WT, de Groot K (1986) Macropore tissue ingrowth: a quantitative and qualitative study on hydroxyapatite ceramic. Biomaterials 7 137-143.

Büsing CM, Zöllner C, Heimke G (1987) The degradation of calcium phosphate ceramics. Clinical Mater. 2 303-307.

Daculsi G, LeGeros RZ, Nery E, Lynch K, Kerebel B (1989) Transformation of biphasic calcium phosphate ceramics in vivo: Ultrastructural and physiochemical characterization. J. Biomed. Mater. Res. 23 883-894.

Davies JE, Matsuda T (1988) Extracellular matrix production by osteoblasts on bioactive substrata in vitro. Scanning Microsc. 2 1445-1452.

Denissen HW, de Groot K, Makkes PC, van den Hooff A, Klopper PJ (1980) Tissue response to dense apatite implants in rats. J. Biomed. Mater. Res. 14 713-721.

DIN 4768, and DIN 4762/1E Maximale Rauhtiefe, Begriffe, Mai 1978, Deutsches Institut für Normung e.V., Berlin, FRG.

de Groot K (1980) Bioceramics consisting of calcium phosphate salts. Biomaterials 1 47-50.

Gross UM, Strunz V (1980) The anchoring of glass-ceramics of different solubility in the femur of the rat. J. Biomed. Mater. Res. 14 607-618.

Gross U, Brandes J, Strunz V, Bab I, Sela J (1981) The ultrastructure of the interface between a glass-ceramic and bone. J. Biomed. Mater. Res. 15 291-305.

Gross U, Strunz V (1985) The interface of various glasses and glass-ceramics with a bony implantation bed. J. Biomed. Mater. Res. 19 251-271.

Gross U, Müller-Mai C, Knarse W, Voigt C (1988a) Structures at the interface of bone-bonding and non-bonding glass-ceramics in the scanning electron microscope. In: BIOMAT 87, Calcified Tissues and Biomaterials. Harmand MF (ed.). Les Publications de Biomat, pp 249-256.

Gross U, Kinne R, Schmitz HJ, Strunz V, (1988b) The response of bone to surface-active glasses/glass-ceramics. CRC Critical Reviews in Biocompatibility, Vol. 4, CRC Press, Boca Raton, Florida, USA, pp 155-179.

Gross U, Müller-Mai C, Fritz T, Voigt C, Knarse W, Schmitz HJ (1989) Implant surface roughness and mode of load transmission influence periimplant bone structure. In: Proc. 8th European conference on Biomaterials, Heidelberg, FRG, Sept. 7-9, 1989, in press.

Hench LL, Splinter RJ, Allen WC, Greenlee TK (1971) Bonding mechanisms at the interface of ceramic prosthetic material. J. Biomed. Mater. Res. 2 117-141.

Hench LL, Ethridge EC (1982) Biomaterials, an interfacial approach. Academic Press, New York, USA.

Hoogendoorn HA, Renoou W, Akkermans LMA, Visser W, Wittebol P (1984) Long-term study of large ceramic implants (porous hydroxyapatite) in dog femora. Clin. Orthop. Rel. Res. 187 281-288.

Jarcho M (1981) Calcium phosphate ceramics as hard tissue prosthetics. Clin. Orthop. Rel. Res. 157 259-278.

Kato K, Aoki H, Eng D, Tabata T, Ogiso M (1979) Biocompatibility of apatite ceramics in mandibles. Biomat. Med. Dev. Art. Org. 7 291-297.

Klein CPAT, Driessen AA, de Groot K, van den Hoof A (1983) Biodegradation behavior of various calcium phosphate materials in bone. J. Biomed. Mater. Res. 17 769-784.

Klein CPAT, de Groot K, Driessen AA, van der Lubbe HBM (1985) Interaction of biodegradable ß-whitlockite ceramics with bone tissue: An in vivo study. Biomaterials 6 189-192.

Klein CPAT, de Groot K, Driessen AA, van der Lubbe HBM (1986) A comparative study of different ß-whitlockite ceramics in rabbit cortical bone with regard to their biodegradation behaviour. Biomaterials 7 144-146.

Köster K, Karbe E, Kramer H, Heide H, König R (1976) Experimenteller Knochenersatz durch resorbierbare Calciumphosphat-Keramik. Langenbecks Arch. Chir. 341 77-86.

Kwong CH, Burns WB, Cheung HS (1989) Solubilization of hydroxyapatite crystals by murine bone cells, macrophages and fibroblasts. Biomaterials 10 579-584.

Matsuda T, Davies JE (1987) The in vitro response of osteoblasts to bioactive glass. Biomaterials 8 275-284.

Müller-Mai C, Schmitz HJ, Strunz V, Fuhrmann G, Fritz T, Gross UM (1989) Tissue at the surface of the new composite material titanium/glass-ceramic for replacement of bone and teeth. J. Biomed. Mater. Res. 23 1149-1168.

Salthouse TN (1984) Some aspects of macrophage behaviour at the implant interface. J. Biomed. Mater. Res. 18 395-401.

Winter M, Griss P, de Groot K, Tagai H, Heimke G, van Dijk HJA, Sawai K (1981) Comparative histocompatibility testing of seven calcium phosphate ceramics. Biomaterials 2 159-161.

DISCUSSION WITH REVIEWERS

J.E. Davies: The term corrosion seems to refer to the relatively well known phenomenon of dissolution of intergrain "neck" regions leading to the release of ceramic grains into the local environment. I feel the term corrosion, in this case, is confusing as it is more usually associated with far less site specific changes in materials (normally metals). For this reason I feel the word "corrosion" should be removed from this manuscript. The author's observations would be the same but the sense would be clearer.

Authors: Although the term "corrosion" has been used mostly for metals a particulate disintegration or corrosion occurs in a wide range of materials. The amount and kind of released particles is determined partially by the material properties, but the result within the tissue is similar, i.e. there are released particles. Therefore, it seems not suitable to create different terms for different materials, e.g. corrosion for metals, degradation for polymers, and other terms for ceramics and HA.

D.E. Steflik: The degradation of hydroxyapatite is an interesting concept. On the premise that this in fact occurs, what do the authors believe is the rate of this degradation? Could the

authors also comment on the commercially available "resorbable" HA materials? What kind of ions do the authors believe are lost if corrosion in fact occurs?
Authors: A quantification of the degradation process is necessary e.g. by measuring pore and grain diameters under controlled circumstances on more implants. The amount of resorbed material could be measured by the method described by A. Boyde and S.J. Jones (Scanning Electron Microscopy, 1979, II, 393-402, Chicago, USA).

Yet, the authors cannot comment on commercial materials, since the investigations with a commercial material started recently. It was demonstrated by other investigators (C.P.A.T. Klein et al.: Dissolubility of calciumphosphate particles in relation to different buffer-solvents, European Intensive Course on Biomaterial Degradation, Oporto, Portugal, Sept. 12-16, 1988) that tricalciumphosphate, tetracalciumphosphate and to a much lower degree HA can dissolve in different aqueous solutions which results in the release of various ions, such as Ca^{++}, PO_4^{3-}, and OH^-. A reprecipitation in the form of HA via other Ca/P-phases seems to be possible and might account for chemical bone-bonding.

D.E. Steflik: In the introduction the authors suggest that surface roughness increases the inflammatory response to these implants. As long as the roughness is kept well below the level of bone, this is not necessarily the case. The authors should defend this comment.
Authors: The citation was given in the context of increased leaching and release of particles (corrosion) which might occur under certain circumstances. Such processes might enhance further dissolution of Ca-containing implants and might delay or hinder bone-bonding. In situations like this the surface roughness becomes important, e.g. due to the increased surface area.

J.E. Davies: Kwong et al., 1989 provided no direct proof of osteoclastic resortion of implant particles. Indeed their experiments did not include implants. In the present paper the authors seem to infer that proof has been reported of specific osteoclastic resorption of implant materials. This is not the case in the reference cited and indeed Kwong et al. fell into the same trap when referencing other authors such as van Blitterswijk who provided clear evidence of juxtaposition to calcium phosphate implants by multinucleate giant cells which had no of the distinguishing features (apart from nuclearity) of osteoclasts.
Authors: It is not inferred by the authors, that osteoclastic resorption has been reported by Kwong et al.. The aim of referencing this paper was to give evidence that some cells are able to solubilize incorporated material after resorption. Some evidence of specific osteoclastic resorption of HA was given in our paper.

J.E. Davies: In several of the specimens you report a layer, most closely apposed to the implant surface, comprising a seam of mineralized fibers covered with a layer of collagen-rich ECM. What do you consider the structure of this seam to be? What is the fiber component of this layer? Is it related to any other mineralized tissue seen in the body? How is this related to the Lamina Limitans reported by Scherft, J.P.: J. Ultrastruct. Res. 64, 173-181, 1978 and associated with some other calcium phosphate implants (van Blitterswijk, C.A. & Grote, J.J.: Crit. Reviews in Biocompat. 5, 13-43, 1989)?
Authors: Using SEM and TEM no differences between the "seam of mineralized fibers" and the surrounding bone were observed. Due to areas of slight decalcification which cannot be avoided totally, a crossbanding of the fiber component was seen which corresponded to this type of collagen fibers. Generally, the layer-like appearence seems to be related to the surface reactivity of the implants since we observed it in a comparable manner around other types of surface-reactive implants, e.g. bone-bonding glass-ceramics. On the other hand, inert implants and non-bonding glass-ceramics did not show this phenomenon. There was no relation to other mineralized tissues in the body or to the Lamina Limitans reported by J.P. Scherft. In this context it must be emphasized, that J.P. Scherft observed the Lamina Limitans in decalcified sections and that the results presented here show sections of undecalcified bone. As described above, zones of slight decalcification could not be avoided totally. Structures with Lamina Limitans-like appearence were sometimes observed in these zones. This points to the importance of the mode of preparation.

D.E. Steflik: How did the authors determine if leaching, corrosion or resorption was specifically occurring? The authors make a good point of the importance of these processes to liberate implant particles that could then be phagocytozed.
Authors: Investigations in using various techniques demonstrated that material surfaces of surface reactive glasses and Ca/P implants or other substances can undergo 1. leaching, i.e. loss of soluble material from the matrix and 2. particulate degradation or corrosion, i.e. loss of particulate material. These processes were observed without cellular interaction by interstitial fluid and/or they can be enhanced by cellular interaction, e.g. by macrophages and osteoclasts which was demonstrated in several parts of this paper.

Reviewer #4: Meaning of table 1 & 2 is rather ambiguous and were there any statistical differences between the two groups (interface and fracture plane, 84 days and 168 days) in table 1 and 2?
D.E. Steflik: The quantification of pore and diameter size is noteworthy. How were the investigators assured that the measurements were representative samples of the HA dimensions? This is important as to verify their claim of decreased grain diameter and increased pore diameter which is a principle claim for the

degradation of the HA material. The tables are unclear as to this general trend.
Authors: Due to the small number of implants there is no sense in performing statistical tests. As mentioned in Materials and Methods and in the Discussion, these data can give a trend only because of the small number of implants and because there is no evidence for the distance between interface and fracture plane within the HA. The increasing pore diameter and the decreasing grain diameter is well in accordance with another study referenced in the Discussion (Daculsi et al., 1989). Controlled leaching experiments are necessary.

J.E. Davies: Figure 9 shows part of an apparently large cell. The two nuclei are not seen as distinct bodies (in some giant cells this could represent a lobed nuclear structure). Why was the photomicrograph cropped in this way?
Authors: In serial sections of this specimen there was no connection between the two nuclei. The photomicrograph was cropped since there was part of the grid covering the upper part of the photomicrograph.

D.E. Steflik: Identification of osteoclasts (Figure 13) by surface morphology SEM of the brush border is difficult. Is not the brush border on the underside of the cell? Please clarify the authors identification of cell type by surface SEM morphology.
Authors: The cell shown in Figure 13 is morphologically similar to migrating rabbit osteoclasts which were demonstrated in time-lapse video observations by T.J. Chambers et al. (J. Cell Sci. 66, 383-399, 1984), since it is of about 50 μm in length, shows a rather smooth cellular membrane with pseudopods on its left side, and a process with filopods on the other side (which might be the edge of a brush border) extending into a newly created pit within the HA implant. According to the observations by T.J. Chambers et al. it is very likely, that the cell in Figure 13 is an osteoclast which migrated to the left of the photomicrograph. Additionally, the scalloped outline of the pit should be noticed, since it is typically for osteoclastic resorption lacunae.

J.E. Davies: The 10 micron pits shown in Figure 14 are quite small and do not possess the "classical" scalloped outline of osteoclastic resorption pits (which is evident in one area of Figure 13). While these pits lie within an area which seems to have been subject to surface "erosion" of some type, can you postulate the size of the cells which may have been responsible for such change in surface morphology? How much will the appearence in this photomicrograph have been influenced by surface defect structures in the HA coating leading to localized surface dissolution or enhancement of dissolution at ceramic grain necks?
Authors: In pits similar to these shown in Figure 14 we have never seen intact cells. In some, we observed remnants of cellular processes which is shown in the left pit of Figure 14. Therefore we cannot postulate the size of the cell. There are hints in the literature which showed lacunae of comparable width and form in devitalized bone slices in vitro which were produced by osteoclasts with diameters of about 20 μm (Shimizu, H. et al.: The effect of substrate composition and condition on resorption by isolated osteoclasts. Bone and Mineral, 6, 261-275, 1989). Since in some of the implants other phases than HA could be detected it might be possible that the pits of Figure 14 are within a zone of inhomogenous surface composition.

Reviewer #4: To clarify this resorption process by osteoclasts, it would be desirable to show the identification of osteoclasts, i.e. histo-chemical analysis (stained positive for tartrate-resistant acid phosphatase activity, etc.). Furthermore, recent report (Shimizu, H. et al.: The effect of substrate composition and condition on resorption by isolated osteoclasts. Bone and Mineral, 6, 261-275, 1989) osteoclasts can adhere to the surface of HA, however, did not resorb the surface of the crystal.
Authors: Histo-chemical stainings of similarly prepared glass-ceramics (KG Cera etc.) were performed already in our laboratory (unpublished data, submitted for publication to Biomaterials). From 2 to 7 days after implantation there was a layer of acid phophatase positive cells on the surface of both, bone-bonding glass-ceramic KG Cera and non-bonding glass-ceramic. In the SEM these cells showed features of macrophages. After longer time intervalls the number of these cells decreased (faster on the surface of the bone-bonding material). Due to the small number of implants it was not possible to apply histochemical techniques in this study.
That resorption of surface reactive implants mediated by cells, e.g. osteoclasts can occur was not only shown in this study (J.E. Davies, 15th Annual Meeting of the Society for Biomaterials, April 1989).

D.E. Steflik: The implant cylinders used in this study were of the dimensions of potential dental implant devices. However, as in numerous studies from the literature, the devices are placed into unloaded sites in long bones. Since the bone dynamics of long bones are different than the bone dynamics of the jaw, could the authors discuss two items? First, what differences would they expect if they placed the implants in the jaw (mandible or maxilla)? Second, what differences would they expect if the implants were subjected to occlusal loading?
Authors: The implants are partially loaded and not unloaded. This will be demonstrated in another report by structural light microscopical results which show totally different bony reactions around inert vs. surface reactive implants and implants with smooth vs. rough surfaces. In answer to the two questions, we like to refer to a study which is referenced in this paper (Müller-Mai et al., 1989). Implants of the composite material titanium/glass-ceramic were examined using the femur model, and using loaded and unloaded (submerged) tooth implants. The results are discussed in detail in this paper.